

Observation of Enhanced Chiral Asymmetries in the Inner-Shell Photoionization of Uniaxially Oriented Methyloxirane Enantiomers

Maurice Tia,^{*,†,‡} Martin Pitzer,^{†,‡} Gregor Kastirke,[†] Janine Gatzke,[†] Hong-Keun Kim,[†] Florian Trinter,[†] Jonas Rist,[†] Alexander Hartung,[†] Daniel Trabert,[†] Juliane Siebert,[†] Kevin Henrichs,[†] Jasper Becht,[†] Stefan Zeller,[†] Helena Gassert,[†] Florian Wiegandt,[†] Robert Wallauer,[†] Andreas Kuhlins,[†] Carl Schober,[†] Tobias Bauer,[†] Natascha Wechselberger,[†] Phillip Burzynski,[†] Jonathan Neff,[†] Miriam Weller,[†] Daniel Metz,[†] Max Kircher,[†] Markus Waitz,[†] Joshua B. Williams,^{†,§} Lothar Ph. H. Schmidt,[†] Anne D. Müller,[‡] André Knie,^{‡,||} Andreas Hans,[‡] Ltaief Ben Ltaief,[‡] Arno Ehresmann,[‡] Robert Berger,^{||} Hironobu Fukuzawa,[⊥] Kiyoshi Ueda,[⊥] Horst Schmidt-Böcking,[†] Reinhard Dörner,[†] Till Jahnke,[†] Philipp V. Demekhin,^{*,‡} and Markus Schöffler^{*,†}

[†]Institut für Kernphysik, Goethe Universität Frankfurt, Max-von-Laue-Straße 1, 60438 Frankfurt am Main, Germany

[‡]Institut für Physik und CINSaT, Universität Kassel, Heinrich-Plett-Straße 40, 34132 Kassel, Germany

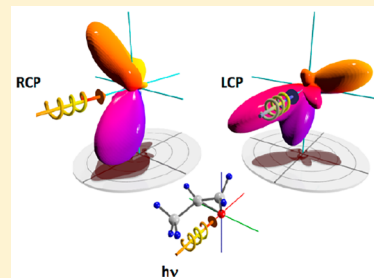
[§]Department of Physics, University of Nevada, Reno, Nevada 89557, United States

^{||}Theoretical Chemistry, Department of Chemistry, Philipps-Universität Marburg, Hans-Meerwein-Straße, 35032 Marburg, Germany

[⊥]Institute of Multidisciplinary Research for Advanced Materials, Tohoku University, Sendai 980-8577, Japan

Supporting Information

ABSTRACT: Most large molecules are chiral in their structure: they exist as two enantiomers, which are mirror images of each other. Whereas the rovibronic sublevels of two enantiomers are almost identical (neglecting a minuscule effect of the weak interaction), it turns out that the photoelectric effect is sensitive to the absolute configuration of the ionized enantiomer. Indeed, photoionization of randomly oriented enantiomers by left or right circularly polarized light results in a slightly different electron flux parallel or antiparallel with respect to the photon propagation direction—an effect termed photoelectron circular dichroism (PECD). Our comprehensive study demonstrates that the origin of PECD can be found in the molecular frame electron emission pattern connecting PECD to other fundamental photophysical effects such as the circular dichroism in angular distributions (CDAD). Accordingly, distinct spatial orientations of a chiral molecule enhance the PECD by a factor of about 10.



Photoionization of unpolarised electronic states of an atom is insensitive to the light's helicity: The count rate on an electron detector placed at any particular angle does not change when switching between photons of different circular polarization. In order to make the photoelectron count rate sensitive to the photon helicity, the measurement conditions need to establish a coordinate frame of specific handedness. Two of the three vectors required to define such a coordinate frame are the k -vector of the photon (i.e., the photon propagation direction) and the k -vector of the photoelectron (i.e., the emission direction). The third vector can be introduced, for instance, by a second photoelectron in the case of photo double ionization, where the observed coincident detection of two electrons depends on the light's helicity.^{1,2} Alternatively, orienting a linear molecule in space can provide an additional (molecular) axis, which results in a prominent effect that depends on the helicity of the light.^{3,4} Results from the well-studied example^{4,5} of the inner-shell ionization of CO are shown in Figure 1a,b. While the photoelectron angular emission distribution possesses a strong asymmetry within the light's polarization

plane (Plane B in Figure 1), the forward/backward symmetry (i.e., the symmetry relative to the photon propagation direction in Plane A) remains.

In the case of molecular photoionization, the shape of the emission distribution results from the scattering of the outgoing electron wave by the molecular ion potential. The circularly polarized light additionally imprints the direction of the rotation of its electric field onto that scattered wave. Because switching the helicity of the light is equivalent to a parity inversion, it results in the inversion of the distribution in Figure 1a along the vertical axis, yielding the emission pattern shown in Figure 1b. The normalized difference of these emission patterns for the two helicities is known as the circular dichroism in angular distributions (CDAD),⁴ and since it is symmetric in

Received: April 24, 2017

Accepted: June 5, 2017

Published: June 5, 2017

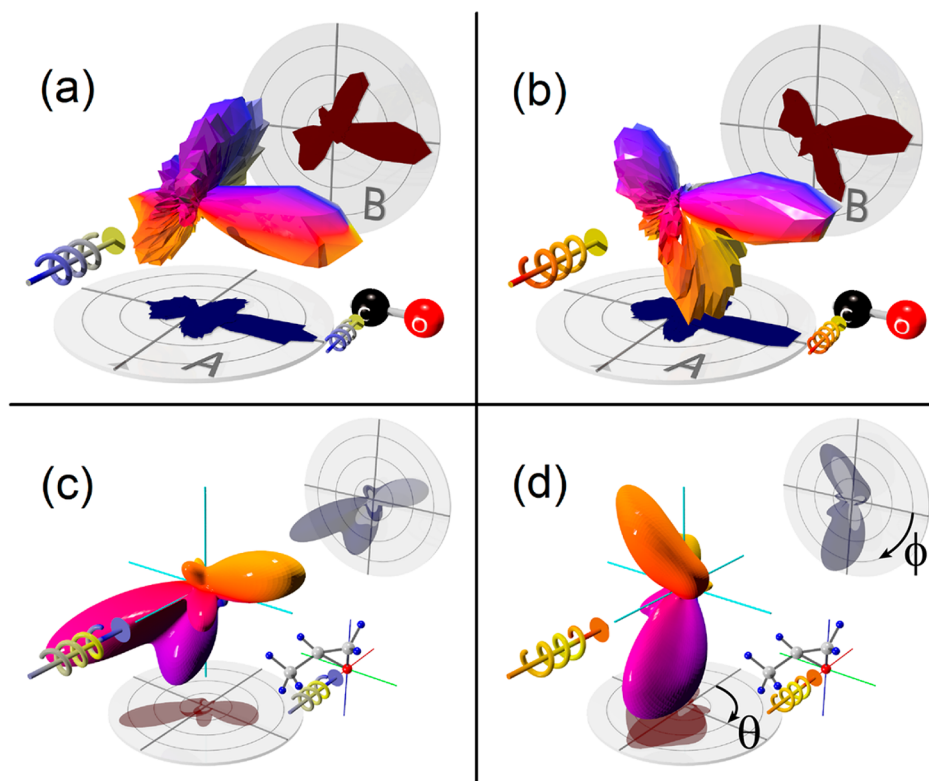


Figure 1. Three-dimensional molecular frame photoelectron angular distributions. Top: for the C 1s-electrons emitted from CO for left (a) and right (b) circularly polarized light (taken from ref 5). Bottom: theoretical distributions computed here for the O 1s-ionization of R(+) methyloxirane by left (c) and right (d) circularly polarized light. The molecules are oriented as depicted in the insets. Polar and azimuthal angles $\{\theta, \phi\}$ are indicated in panel d.

the forward/backward directions, it depends only on the azimuthal angle ϕ around the light propagation:⁵

$$\text{CDAD} = \frac{I_{+1}(\phi) - I_{-1}(\phi)}{I_{+1}(\phi) + I_{-1}(\phi)}$$

Here I_{+1} and I_{-1} correspond to the ionization cross section by left or right circularly polarized light (labeled by positive or negative helicity ± 1). The asymmetry of the electron flux induced by circularly polarized photons in the up/down directions has been successfully utilized, e.g., in surface science to stereoscopically image nearest neighbor distances.⁶ For molecules that are “fixed-in-space”, CDAD values up to 100% can be observed.⁵

A forward/backward asymmetry in the photoemission—even within the electric-dipole approximation⁷—can arise due to scattering of the electron wave by the molecular potential whenever the structure of a fixed-in-space molecule breaks that symmetry. The change of this forward/backward asymmetry in the emission distribution that arises when switching the light’s helicity is termed photoelectron circular dichroism (PECD). PECD occurs as the molecular structure acts as the gearbox, which translates the rotation of the electric field vector into a change of the forward (or backward) directed electron flux. A mechanical analogue for such machinery is a nut on a thread. The thread transforms the rotation of the nut into forward (or backward) directed motion. Figure 1c,d shows the corresponding effect on the molecular level: our calculated electron emission patterns from fixed in space R(+) methyloxirane ($\text{C}_3\text{H}_6\text{O}$) show dramatic changes upon switching the light helicity and thus substantial PECD. Furthermore, from these

figures it becomes intuitively understandable, that PECD is sensitive to subtle changes of the molecular potential (shape and structure), both static^{8–14} and dynamic.¹⁵

Only for nonracemic chiral molecules is a PECD even observable after averaging over all possible molecular orientations,^{16,17} while for achiral molecules all asymmetries cancel out for a sample of randomly oriented molecules. This is due to the fact that, for achiral molecules, the mirror image of any molecular orientation can be created by a rotation, and, by definition, the PECD value has the opposite sign for the mirror image. For nonracemic chiral molecules on the contrary, the cancelation can be incomplete, as the mirror situation with the opposite sign of the PECD equals a switch of enantiomers and thus cannot be generated by a rotation. In the past decade, PECD for randomly oriented molecules has been invoked as a powerful chiroptical tool to enable determination of the absolute configuration of chiral molecules.^{18–20} PECD has also been speculated to be one of the symmetry-breaking mechanisms at the origin of life’s homochirality.¹¹

Recently, the first laser-based PECD measurements^{21–24} have further demonstrated their potential as analytical applications for characterization of chiral pharmaceuticals. In multiphoton experiments on chiral molecules, additional dichroic effects due to the intermediate state alignment can be produced. Especially, in the case of nonresonant two-photon excitation, an orientation-dependent probability distribution of the molecules in the resonant intermediate state can be observed. For example, the model described by Goetz et al.²⁵ of one-photon photoionization of an initial state prepared by nonresonant, orientation-dependent two-photon absorption shows PECD values up to 35%. Sen et al. also observed

dichroic features in resonance-enhanced two-photon ionization of achiral nitric oxide molecules.²⁶ Additionally, by performing experiments and calculations in the time domain, the intermediate state structure and dynamics and possible nonradiative relaxation pathways could also be investigated. Furthermore, Comby et al. have demonstrated that time-resolved PECD could be used as a sensitive probe of ultrafast dynamics in chiral molecules with femtosecond resolution.²⁷

While it has already been suggested that the scattering of the photoelectron wave at the molecular potential is at the heart of PECD,^{16,28,29} the validity of this intuitive picture has so far not been demonstrated directly, for example, by performing experiments on spatially oriented molecules. Contrarily, to date, PECD in the gas phase has only been studied for randomly oriented molecules. Accordingly, the observed effect is comparably weak in those studies. A typical magnitude of the normalized difference,²⁸ $PECD = \frac{I_{+1}(\theta) - I_{-1}(\theta)}{I_{+1}(\theta) + I_{-1}(\theta)}$, where θ is the polar emission angle of the electron with respect to the light propagation, was on the order of a few percent, because integration over all molecular orientations drastically reduces the contrast and thus lowers the PECD values. Note that several definitions of PECD exist in literature, and the present PECD refers to the dichroic parameter b_1 , which is half of the routinely used $2b_1$.

Our calculations shown in Figure 1c,d demonstrate that PECD occurring for certain molecular orientations is strongly enhanced and in principle could reach 100%. In order to verify this prediction experimentally, one would need to fix the orientation of the examined molecule in space, or alternatively measure the molecular orientation at the instant of photoemission. The present work makes a major step toward this goal by choosing the latter approach and studying uniaxially oriented methyloxirane molecules upon O (1s)-photoionization ($h\nu = 550$ eV) using the COLTRIMS-technique.³⁰ A specially designed high-resolution (3d focusing for electrons and ions) spectrometer without any meshes in order to increase the overall particle detection efficiency has been employed. The peak of observed photoelectrons was centered at a kinetic energy of about 11.5 eV. Before the nuclei start to rearrange in response to the creation of the O (1s)-hole, an ultrafast Auger decay takes place, which is finally followed by a Coulomb fragmentation of the doubly charged ion. Even though fragments with a mass over charge ratio m/z equal to 14, 15, 25, 26, 27, 28, 29, 30, 31, and 42 have been observed in the photoion-photoion coincidence (PIPICO) spectra, the present analysis was performed only for two types of molecular breakup with the following fragment combinations: $C_2H_2^+(m/z 26)$ – $COH^+(m/z 29)$ and $CH_3^+(m/z 15)$ – $C_2H_2O^+(m/z 42)$. The COLTRIMS technique provides the momenta of all charged reaction products. While it is in most cases straightforward to deduce the molecular orientation from the measured ion momenta for small, diatomic molecules, it is not trivial to relate the measured asymptotic momenta of the ionic fragments to a given molecular axis for a larger molecule. Therefore, the molecular orientation at the instant of the photoionization was an optimization parameter in the present electronic structure and dynamic calculations, which were carried out by the single center method and code.^{31,32} Details on the experimental approach and the theory can be found in the Supporting Information.³³

Figure 2 compares the measured and computed PECD for randomly oriented molecules (a) and for the two cases where

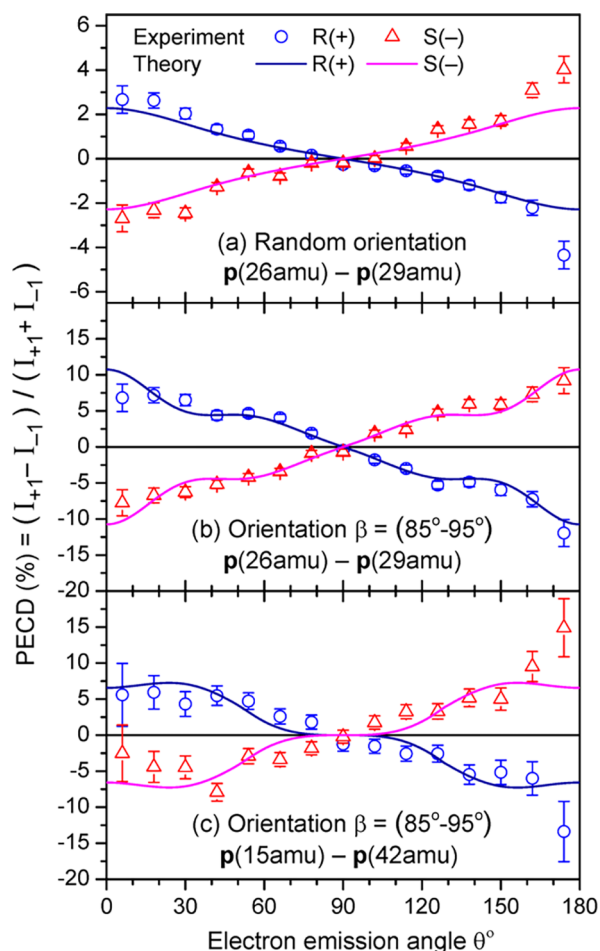


Figure 2. PECD as a function of the photoelectron emission angle θ , with respect to the photon propagation, measured and computed in the present work for the O 1s-photoionization of the two enantiomers of methyloxirane: (a) for randomly oriented molecules and p(26 amu)–p(29 amu) fragmentation channel and (b,c) for the fragmentation axis being fixed at an angle $\beta = 90^\circ$ with respect to the light propagation direction and for the two different fragmentation channels p(26 amu)–p(29 amu) and p(15 amu)–p(42 amu).

the fragmentation axis of the molecules was fixed-in-space (b and c). In this work, the electrons were gated on the photoelectron peak centered at 11.5 eV kinetic energy. The PECD measured for the randomly oriented molecules (note that Figure 2a comprises only data for the p(26 amu)–p(29 amu) channel) shows maximum values between 3% and 4%, whereas the PECD obtained after fixing the fragmentation axes in space parallel to the polarization plane (the angle between the fragmentation axis and the light propagation axis was between 85 and 95°) shows much higher asymmetries (Figure 2b,c). In particular, applying such a restriction to the fragmentation channel p(26 amu)–p(29 amu) gives experimental asymmetry values up to 12%, whereas theoretical curves lead to the maximum asymmetry of 10%. Similar enhancement is observed for the fragmentation channel p(15 amu)–p(42 amu). We also note that the generally expected change of sign of PECD with respect to the interchange of the enantiomers (R(+) and S(–) denote the two different enantiomers) is clearly observed for both randomly oriented and fixed-in-space molecules.

A more detailed view of the PECD is given in Figures 3 and 4. These figures depict PECDs obtained for the two

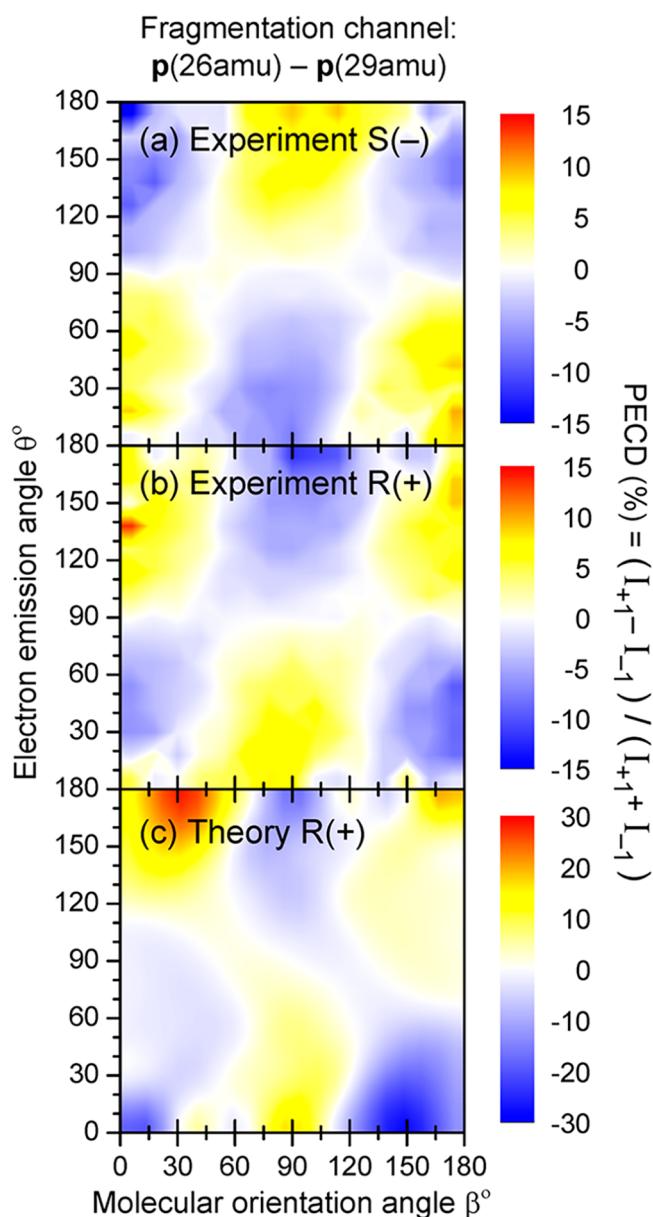


Figure 3. PECD as a function of the photoelectron emission angle θ and the molecular orientation angle β after O 1s-photoionization and subsequent dissociation of methyloxirane into p(26 amu) and p(29 amu) fragments: (a) measurements for the S(–) enantiomer; (b) measurements for the R(+) enantiomer; (c) calculations for the R(+) enantiomer. Note that PECD computed for the S(–) enantiomer (not shown here) has an opposite sign. For the sake of brevity, orientation of the molecular fragmentation axis in space is shortly referred to throughout as the molecular orientation.

fragmentation channels as functions of the photoelectron emission angle θ and of the molecular orientation angle β (angle between the fragmentation axis and the light propagation). One can see, as well, that the sign of the PECD changes when the enantiomers are swapped (cf., Figure 3a,b and Figure 4a,b). This latter finding confirms that the observed asymmetry has a chiral origin. Moreover, the measured two-dimensional PECDs confirm the following analytically derived symmetry property: $\text{PECD}(\pi - \theta; \pi - \beta) = -\text{PECD}(\theta; \beta)$. Since we observe different signs of PECD upon switching between the forward ($\theta = 0^\circ$) and the backward ($\theta = 180^\circ$) photoemission directions, the symmetry rule results

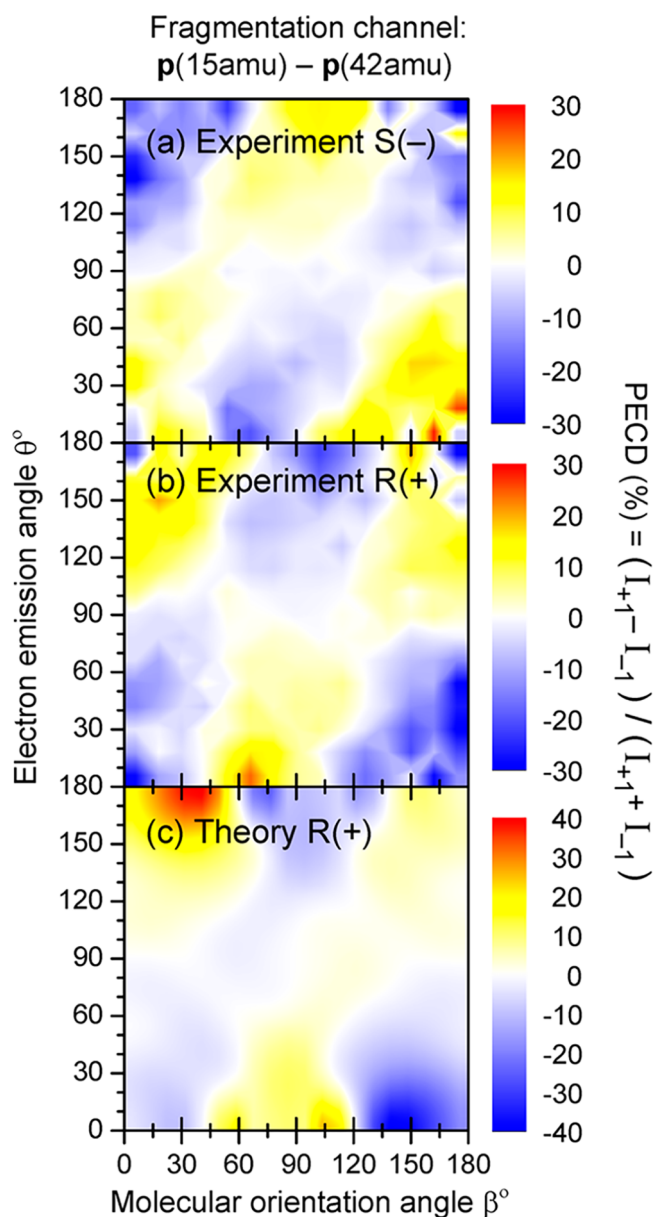


Figure 4. Same as in Figure 3 but for the p(15 amu)–p(42 amu) fragmentation channel.

in similar signs for the molecular axis oriented along the light propagation ($\beta = 0^\circ$, forward) and in the reversed direction ($\beta = 180^\circ$, backward). For a given enantiomer, the PECD reverses its sign when the molecular orientation changes from being parallel to the light propagation axis ($\beta = 0/180^\circ$) to the case when it is orthogonal to the light propagation ($\beta = 90^\circ$). Therefore, integration over all orientations results in a considerably smaller effect.

Experimentally, we find an asymmetry of up to 15% for the p(26 amu)–p(29 amu) breakup and even higher asymmetries up to 30% in the case where ($\theta = 0^\circ$; $\beta = 160^\circ$) for the fragmentation channel p(15 amu)–p(42 amu). The higher asymmetry observed at some molecular orientations for the latter fragmentation channel can be explained by the fact that it corresponds to a single bond breaking (loss of methyl group), whereas the former requires the breaking of two bonds. As a consequence, the analysis of the coincident data allows for a more accurate determination of the molecular orientation for

the p(15 amu)–p(42 amu) breakup, whereas in the case of the p(26 amu)–p(29 amu) channel, an additional averaging over orientations can be present. The computed PECDs (Figures 3c and 4c) show a good overall agreement with the experimental data: Both have similar signs of asymmetries, but the theoretical values are somewhat overestimated. For the fragmentation channel p(26 amu)–p(29 amu), the calculations show asymmetries up to 30%, whereas a PECD of about 35% is computed for the fragmentation channel p(15 amu)–p(42 amu). Integration of the signals $I_{\pm 1}$ over all angles β gives the much smaller PECD observed for randomly oriented samples (Figure 2a). Finally, the dichroic parameter b_1 computed and measured for the R(+) enantiomer is very small and equals to 1.35% and $1.56\% \pm 0.25\%$, respectively. These results support the intuitive prediction that selecting a particular 3D orientation, rather than averaging over all orientations, enables removal of any cancellation that occurs due to compensation of the PECD for different molecular orientations.

As PECD depends only on the angle θ with respect to the light propagation axis, we have so far averaged the electron distribution over the azimuthal angle ϕ . By selecting molecular orientations to be perpendicular to the light propagation direction ($\beta = 90^\circ$), the CDAD as a function of the azimuthal emission angle ϕ in the polarization plane can be extracted from the experimental coincident data. The measured CDADs are depicted in Figure 5. Unlike PECD, which have different signs for the two enantiomers, the CDAD is enantiomer insensitive, having equal trends for R(+) and S(–) methyloxirane. Accordingly, the CDAD has to vanish for randomly oriented chiral molecules, similarly to the case of randomly

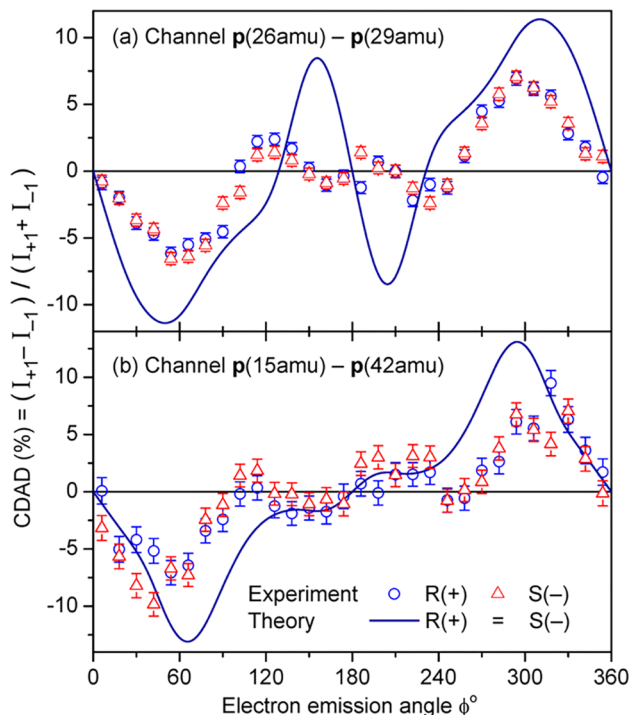


Figure 5. CDAD as a function of the azimuthal photoelectron emission angle ϕ in the polarization plane, measured and computed for the O 1s-photoionization of two enantiomers of methyloxirane and the two fragmentation channels: (a) p(26 amu)–p(29 amu), and (b) p(15 amu)–p(42 amu). Note that CDAD computed for R(+) and S(–) enantiomers are equivalent. Electrons are selected in the range $0^\circ < \theta < 180^\circ$ and ions in the range $85^\circ < \beta < 95^\circ$.

oriented achiral molecules. Finally, the computed CDADs reproduce the trends of the experimental asymmetry, although the theory slightly overestimates its magnitude (Figure 5). One can note that the CDAD and the PECD were obtained by two very different data treatments (see Supporting Information³³ for details). This can be a reason for the larger disagreement between the theory and experiment for the CDAD, since building a new coordinate system for the data analysis could result in larger uncertainties of the emission and the orientation angles determination. The observed discrepancy therefore exceeds the purely statistical error bars shown in Figure 5.

In conclusion, all previous studies of PECD in the gas phase were performed for randomly oriented chiral molecules. In those studies, the PECD was discussed in terms of laboratory frame angular distribution and described as a forward/backward asymmetry in the photoelectron emission which survives after averaging over all molecular orientations. Our theoretical predictions illustrate that fixing three-dimensional orientation of a target in space may in principle result in a 100% effect, as it is known for CDAD. Using coincident detection technique, we provide the first experimental proof for those expectations and demonstrate that chiral asymmetry for O(1s)-photoionization of methyloxirane can be significantly enhanced already by fixing one molecular fragmentation axis. Providing larger asymmetries makes the PECD of oriented chiral molecules a more sensitive tool for the enantiomeric excess determination. The present analysis supports the transparent picture of the photoelectron scattering on the molecular potential being at the heart of the PECD. By interrelating the fundamental PECD and CDAD phenomena with the molecular frame photoelectron angular distribution, we pave the way for a detailed understanding of the origin of this fundamental photo physical effect.

EXPERIMENTAL METHOD

The experiment was performed using the well-established COLTRIMS (Cold Target Recoil Ion Momentum Spectroscopy) technique³⁰ during the 8-bunch mode (pulsed-operation) at the Synchrotron SOLEIL (Saint-Aubin, France). A supersonic expansion of enantiopure methyloxirane molecules (Aldrich, 98% purity) is skimmed to form a molecular beam that crosses the synchrotron radiation provided by the variable polarization undulator-based beamline SEXTANTS. The charged fragments resulting from the Coulomb explosion and the photoelectrons are accelerated in opposite directions perpendicular to the molecular and photon beams by a static electric field (124 V/cm) onto two position and time sensitive multichannel plate detectors (MCPs) with delay line multihit readout and an acceptance angle of 4π for the electrons and ions. From the position of impact onto the detectors, the known distance between the ionization region and the MCPs, and the time-of-flight, the particle trajectories can be calculated and the momentum vector of each particle determined. In our measurement, we have observed and gated our data on the photoelectron peak at 11.5 eV of kinetic energy. Fast Auger electrons that could have been detected—although their solid angle of detection is very small—are therefore discriminated. Only photoelectrons detected in coincidence with two positive ions are considered in this paper. Approximately 2×10^6 events were obtained for the fragmentation channel p(26 amu)–p(29 amu) and 3×10^5 events for the fragmentation channel p(15 amu)–p(42 amu) for a given enantiomer and a given helicity of the light.

THEORETICAL METHOD

In order to describe the O 1s-photoionization of the methyloxirane enantiomers, we applied the *ab initio* theoretical approach developed in our previous angle-resolved studies of the core-excited diatomic^{34–36} and polyatomic molecules.^{37–39} The electronic structure and dynamics calculations were carried out by the Single Center method and code,^{31,32} which provides an accurate description of the partial photoelectron continuum waves in molecules. The photoionization transition amplitudes were computed in the relaxed-core Hartree–Fock approximation including monopole relaxation of the molecular orbitals in the field of the core-vacancy. The calculations were performed at the equilibrium⁴⁰ internuclear geometry of the ground electronic state of methyloxirane.

ASSOCIATED CONTENT

Supporting Information

The Supporting Information is available free of charge on the ACS Publications website at DOI: 10.1021/acs.jpcllett.7b01000.

Details of the experimental procedure and theoretical calculations performed in this work (PDF)

AUTHOR INFORMATION

Corresponding Authors

*E-mail: tia@atom.uni-frankfurt.de.

*E-mail: demekhin@physik.uni-kassel.de.

*E-mail: schoeffler@atom.uni-frankfurt.de.

ORCID

Maurice Tia: 0000-0001-6060-1586

André Knie: 0000-0002-2208-8838

Author Contributions

The experiment was conceived by M.S. and R.D. The experiment was prepared and carried out by M.T., M.P., G.K., J.G., H.–K. K., F.T., J.R., A.H., D.T., J.S., K.H., J.B., S.Z., H.G., F.W., R.W., A.Ku., C.S., T.B., N.W., P.B., J.N., M.W., D.M., M.K., M.W., J.B.W., A.Kn., A.H., L.B.L., H.F., K.U., R.B., and M.S. Data analysis was performed by M.T., M.P., and M.S. Theoretical calculations were performed by P.V.D. and A.D.M. M.T., T.J., P.V.D., R.D., and M.S. wrote the paper. All authors discussed the results and commented on the manuscript.

Notes

The authors declare no competing financial interest.

ACKNOWLEDGMENTS

The work was supported by the State of Hesse Initiative for the Development of Scientific and Economic Excellence (LOEWE) within the focus-project Electron Dynamics of Chiral Systems (ELCH). Financial support by the Deutsche Forschungsgemeinschaft (DFG Projects No. DE 2366/1-1 and DO 604/26-1) is gratefully acknowledged. We thank the staff of SOLEIL for running the facility and providing beamtimes under project 20140056 and 20141178 and especially SEXTANTS beamline for their excellent support. M. S. gratefully acknowledges support by the Adolf Messer foundation. H.F. and K.U. are grateful for support from the X-ray Free Electron Laser Priority Strategy Program of MEXT and from IMRAM, Tohoku University. We thank Thomas Baumert for suggesting to us the nut/thread analogy, which was originally discussed by Ivan Powis in ref 17. We thank T. Daniel Crawford for providing us with the optimized geometry of methyloxirane.

REFERENCES

- (1) Berakdar, J.; Klar, H. Circular dichroism in double photoionization. *Phys. Rev. Lett.* **1992**, *69*, 1175–1177.
- (2) Mergel, V.; Achler, M.; Dörner, R.; Khayyat, K.; Kambara, T.; Awaya, Y.; Zoran, V.; Nyström, B.; Spielberger, L.; McGuire, J. H.; et al. Helicity Dependence of the Photon-Induced Three-Body Coulomb Fragmentation of Helium Investigated by Cold Target Recoil Ion Momentum Spectroscopy. *Phys. Rev. Lett.* **1998**, *80*, 5301–5304.
- (3) Ritchie, B. Theoretical studies in photoelectron spectroscopy. Molecular optical activity in the region of continuous absorption and its characterization by the angular distribution of photoelectrons. *Phys. Rev. A: At., Mol., Opt. Phys.* **1975**, *12*, S67–S74.
- (4) Dubs, R. L.; Dixit, S. N.; McKoy, V. Circular-dichroism in photoelectron angular-distributions from oriented linear-molecules. *Phys. Rev. Lett.* **1985**, *54*, 1249–1251.
- (5) Jahnke, T.; Weber, T.; Landers, A. L.; Knapp, A.; Schossler, S.; Nickles, J.; Kammer, S.; Jagutzki, O.; Schmidt, L.; Czasch, A.; et al. Circular dichroism in K-shell ionization from fixed-in-space CO and N₂ molecules. *Phys. Rev. Lett.* **2002**, *88*, 073002.
- (6) Daimon, H. Stereoscopic Microscopy of Atomic Arrangement by Circularly Polarized-Light Photoelectron Diffraction. *Phys. Rev. Lett.* **2001**, *86*, 2034–2037.
- (7) The asymmetry therefore exists without the need to invoke weaker higher order radiation–molecule interaction terms.
- (8) Di Tommaso, D.; Stener, M.; Fronzoni, G.; Decleva, P. Conformational effects on circular dichroism in the photoelectron angular distribution. *ChemPhysChem* **2006**, *7*, 924–934.
- (9) Turchini, S.; Catone, D.; Contini, G.; Zema, N.; Irrera, S.; Stener, M.; Di Tommaso, D.; Decleva, P.; Prosperi, T. Conformational Effects in Photoelectron Circular Dichroism of Alaninol. *ChemPhysChem* **2009**, *10*, 1839–1846.
- (10) Turchini, S.; Catone, D.; Zema, N.; Contini, G.; Prosperi, T.; Decleva, P.; Stener, M.; Rondino, F.; Piccirillo, S.; Prince, K. C.; Speranza, M. Conformational Sensitivity in Photoelectron Circular Dichroism of 3-Methylcyclopentanone. *ChemPhysChem* **2013**, *14*, 1723–1732.
- (11) Tia, M.; Cunha de Miranda, B.; Daly, S.; Gaie-Levrel, F.; Garcia, G.; Powis, I.; Nahon, L. Chiral asymmetry in the photoionization of gas-phase amino-acid alanine at Lyman- α radiation wavelength. *J. Phys. Chem. Lett.* **2013**, *4*, 2698–2704.
- (12) Tia, M.; Cunha de Miranda, B.; Daly, S.; Gaie-Levrel, F.; Garcia, G. A.; Nahon, L.; Powis, I. VUV Photodynamics and Chiral Asymmetry in the Photoionization of Gas Phase Alanine Enantiomers. *J. Phys. Chem. A* **2014**, *118*, 2765–2779.
- (13) Powis, I.; Daly, S.; Tia, M.; Cunha de Miranda, B.; Garcia, G. A.; Nahon, L. A photoionization investigation of small, homochiral clusters of glycidol using circularly polarized radiation and velocity map electron-ion coincidence imaging. *Phys. Chem. Chem. Phys.* **2014**, *16*, 467–476.
- (14) Daly, S.; Tia, M.; Garcia, G. A.; Nahon, L.; Powis, I. The Interplay Between Conformation and Absolute Configuration in Chiral Electron Dynamics of Small Diols. *Angew. Chem.* **2016**, *128*, 11220–11224.
- (15) Garcia, G.; Nahon, L.; Daly, S.; Powis, I. Vibrationally induced inversion of photoelectron forward-backward asymmetry in chiral molecule photoionization by circularly polarized light. *Nat. Commun.* **2013**, *4*, 2132.
- (16) Ritchie, B. Theory of the angular distribution of photoelectrons ejected from optically active molecules and molecular negative ions. II. *Phys. Rev. A: At., Mol., Opt. Phys.* **1976**, *14*, 359–362.
- (17) Powis, I. Photoelectron Circular Dichroism in Chiral Molecules. *Adv. Chem. Phys.* **2008**, *138*, 267–329.
- (18) Böwering, N.; Lischke, T.; Schmidtke, B.; Müller, N.; Khalil, T.; Heinzmann, U. Asymmetry in photoelectron emission from chiral molecules induced by circularly polarized light. *Phys. Rev. Lett.* **2001**, *86*, 1187–1190.
- (19) Garcia, G. A.; Nahon, L.; Lebeck, M.; Houver, J. C.; Doweck, D.; Powis, I. Circular dichroism in the photoelectron angular distribution

from randomly oriented enantiomers of camphor. *J. Chem. Phys.* **2003**, *119*, 8781–8784.

(20) Turchini, S.; Zema, N.; Contini, G.; Alberti, G.; Alagia, M.; Stranges, S.; Fronzoni, G.; Stener, M.; Decleva, P.; Prospero, T. Circular dichroism in photoelectron spectroscopy of free chiral molecules: Experiment and theory on methyl-oxirane. *Phys. Rev. A: At., Mol., Opt. Phys.* **2004**, *70*, 014502.

(21) Lux, C.; Wollenhaupt, M.; Bolze, T.; Liang, Q. Q.; Kohler, J.; Sarpe, C.; Baumert, T. Circular Dichroism in the Photoelectron Angular Distributions of Camphor and Fenchone from Multiphoton Ionization with Femtosecond Laser Pulses. *Angew. Chem., Int. Ed.* **2012**, *51*, 5001–5005.

(22) Lehmann, C. S.; Ram, N. B.; Powis, I.; Janssen, M. H. M. Imaging photoelectron circular dichroism of chiral molecules by femtosecond multiphoton coincidence detection. *J. Chem. Phys.* **2013**, *139*, 234307.

(23) Fanood, M. M. R.; Ram, N. B.; Lehmann, C. S.; Powis, I.; Janssen, M. H. M. Enantiomer-specific analysis of multi-component mixtures by correlated electron imaging-ion mass spectrometry. *Nat. Commun.* **2015**, *6*, 7511.

(24) Ferré, A.; Handschin, C.; Dumergue, M.; Burgy, F.; Comby, A.; Descamps, D.; Fabre, B.; Garcia, G. A.; Géneaux, R.; Merceron, L.; et al. A table-top ultrashort light source in the extreme ultraviolet for circular dichroism experiments. *Nat. Photonics* **2015**, *9*, 93–98.

(25) Goetz, R. E.; Isaev, T. A.; Nikoobakht, B.; Berger, R.; Koch, C. P. Theoretical description of circular dichroism in photoelectron angular distributions of randomly oriented chiral molecules after multiphoton photoionization. *J. Chem. Phys.* **2017**, *146*, 024306.

(26) Sen, A.; Pratt, S. T.; Reid, K. L. Circular dichroism in photoelectron images from aligned nitric oxide molecules. *J. Chem. Phys.* **2017**, *147*, 013927.

(27) Comby, A.; Beaulieu, S.; Boggio-Pasqua, M.; Descamps, D.; Légaré, F.; Nahon, L.; Petit, S.; Pons, B.; Fabre, B.; Mairesse, Y.; et al. Relaxation Dynamics in Photoexcited Chiral Molecules Studied by Time-Resolved Photoelectron Circular Dichroism: Toward Chiral Femtochemistry. *J. Phys. Chem. Lett.* **2016**, *7*, 4514–4519.

(28) Hergenbahn, U.; Rennie, E. E.; Kugeler, O.; Marburger, S.; Lischke, T.; Powis, I.; Garcia, G. Photoelectron circular dichroism in core level ionization of randomly oriented pure enantiomers of the chiral molecule camphor. *J. Chem. Phys.* **2004**, *120*, 4553–4556.

(29) Stener, M.; Fronzoni, G.; Di Tommaso, D.; Decleva, P. Density functional study on the circular dichroism of photoelectron angular distribution from chiral derivatives of oxirane. *J. Chem. Phys.* **2004**, *120*, 3284–3296.

(30) Ullrich, J.; Moshhammer, R.; Dorn, A.; Dorner, R.; Schmidt, L. P. H.; Schmidt-Bocking, H. Recoil-ion and electron momentum spectroscopy: reaction-microscopes. *Rep. Prog. Phys.* **2003**, *66*, 1463–1545.

(31) Demekhin, P. V.; Ehresmann, A.; Sukhorukov, V. L. Single center method: A computational tool for ionization and electronic excitation studies of molecules. *J. Chem. Phys.* **2011**, *134*, 024113.

(32) Galitskiy, S. A.; Artemyev, A. N.; Jänkälä, K.; Lagutin, B. M.; Demekhin, P. V. Hartree-Fock calculation of the differential photoionization cross sections of small Li clusters. *J. Chem. Phys.* **2015**, *142*, 034306.

(33) See [Supporting Information](#).

(34) Demekhin, P. V.; Petrov, I. D.; Sukhorukov, V. L.; Kielich, W.; Reiss, P.; Hentges, R.; Haar, I.; Schmoranzer, H.; Ehresmann, A. Interference effects during the Auger decay of the C*O 1s⁻¹π* resonance studied by angular distribution of the CO⁺(A) photoelectrons and polarization analysis of the CO⁺(A-X) fluorescence. *Phys. Rev. A: At., Mol., Opt. Phys.* **2009**, *80*, 063425.

(35) Demekhin, P. V.; Petrov, I. D.; Sukhorukov, V. L.; Kielich, W.; Reiss, P.; Hentges, R.; Haar, I.; Schmoranzer, H.; Ehresmann, A. Erratum: Interference effects during the Auger decay of the C*O 1s⁻¹π* resonance studied by angular distribution of the CO⁺(A) photoelectrons and polarization analysis of the CO⁺(A-X) fluorescence. *Phys. Rev. A: At., Mol., Opt. Phys.* **2010**, *81*, 069902.

(36) Demekhin, P. V.; Petrov, I. D.; Sukhorukov, V. L.; Kielich, W.; Knie, A.; Schmoranzer, H.; Ehresmann, A. Symmetry-Forbidden Electronic State Interference Observed in Angularly Resolved NO⁺(A ¹Π) Deexcitation Spectra of the N*O(2σ⁻¹2π²) Resonance. *Phys. Rev. Lett.* **2010**, *104*, 243001.

(37) Knie, A.; Ilchen, M.; Schmidt, P.; Reiß, P.; Ozga, C.; Kambs, B.; Hans, A.; Müglich, N.; Galitskiy, S. A.; Glaser, L.; et al. Angle-resolved study of resonant Auger decay and fluorescence emission processes after core excitations of the terminal and central nitrogen atoms in N₂O. *Phys. Rev. A: At., Mol., Opt. Phys.* **2014**, *90*, 013416.

(38) Antonsson, E.; Patanen, M.; Nicolas, C.; Benkoula, S.; Neville, J. J.; Sukhorukov, V. L.; Bozek, J. D.; Demekhin, P. V.; Miron, C. Dynamics of the C 1s→π* excitation and decay in CO₂ probed by vibrationally and angularly resolved Auger spectroscopy. *Phys. Rev. A: At., Mol., Opt. Phys.* **2015**, *92*, 042506.

(39) Knie, A.; Patanen, M.; Hans, A.; Petrov, I. D.; Bozek, J. D.; Ehresmann, A.; Demekhin, P. V. Angle-Resolved Auger Spectroscopy as a Sensitive Access to Vibronic Coupling. *Phys. Rev. Lett.* **2016**, *116*, 193002.

(40) Tam, M. C.; Russ, N. J.; Crawford, T. D. Coupled cluster calculations of optical rotatory dispersion of (S)-methyloxirane. *J. Chem. Phys.* **2004**, *121*, 3550–3557.